Enhancing Optical Up-Conversion Through Electrodynamic Coupling with Ancillary Chromophores
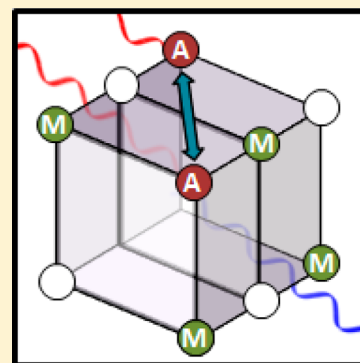
Jamie M. Leeder and David L. Andrews*

School of Chemistry, University of East Anglia, Norwich NR4 7TJ, U.K.

ABSTRACT: In lanthanide-based optical materials, control over the relevant operating characteristics—for example transmission wavelength, phase and quantum efficiency—is generally achieved through the modification of parameters such as dopant/host combination, chromophore concentration and lattice structure. An alternative avenue for the control of optical response is through the introduction of secondary, codoped chromophores. Here, such secondary centers act as mediators, commonly bridging the transfer of energy between primary absorbers of externally sourced optical input and other sites of frequency-converted emission. Utilizing theoretical models based on experimentally feasible, three-dimensional crystal lattice structures; a fully quantized theoretical framework provides insights into the locally modified mechanisms that can be implemented within such systems. This leads to a discussion of how such effects might be deployed to either enhance, or potentially diminish, the efficiency of frequency up-conversion.

INTRODUCTION

In optics, up-conversion (UC) is a broad term applicable to any process enabling a transformation of relatively long wavelength radiation (typically near-infrared) to shorter wavelengths, i.e., higher optical frequencies. In the case of laser radiation, such conversion is commonly achieved through a coherent nonlinear interaction such as second harmonic generation—a capacity widely used for frequency doubling. The materials in which this process occurs are usually optically transparent at the relevant input and output wavelengths, and as such can operate to effect frequency up-conversion without engaging real electronic excitations: generally, these systems require high levels of input intensity. However, other mechanisms can be effectual for the emission of up-converted radiation, at lower levels of input. These are typically noncoherent, stepwise processes, usually entailing resonant absorption of two photons; up-converted emission results from a mechanism involving one or more resonance energy transfer (RET) events. The latter kind of mechanism has widespread applications, as for example in materials for energy harvesting,[1−3] biological imaging and photodynamic therapy[4−6] and solid-state lighting.[7−9] It is therefore not surprising to find considerable interest in methods to control the up-conversion process—the focus of this study is a strategy based on usage of ancillary, nonresonant dopants.

In many of the optical systems whose operation hinges on up-conversion, the key optical centers or chromophores are trivalent rare-earth metal ions. Optical materials based on these ions possess unique properties centered upon their density of accessible electronic levels, and extremely narrow line-width transitions. The ions are typically doped into inorganic glass or crystalline structures, affording chemical and optical stability far superior to most organic materials. Relevant optical emission properties are influenced by local electronic interactions,

determined by the dopant/host combinations, ion concentrations, and atom-scale spatial arrangements—the detailed local atomic or molecular structure of the host is itself significant in determining bulk optical characteristics.[10−13] Past theoretical treatments of up-conversion have considered the detailed role and means of controlling this vicinal electromagnetic environment on UC in lanthanide-based systems, through the relative positioning and interaction of active optical centers.[14,15] The current report instead investigates the role of the local electromagnetic environment on up-conversion, as affected by the relative position and passive interaction with surrounding matter.

It is important to distinguish between active and passive participation of secondary ions or chromophores in these optical materials. Crystalline $NaYF_4$, codoped with Yb^{3+} and Er^{3+} ions, provides a well-characterized example of the former system. The Yb^{3+} ion possesses a relatively long-lived ($\sim 10^{-3}$ s) $2F_{5/2}$ state (with corresponding $2F_{7/2} \rightarrow 2F_{5/2}$ absorption transition) exhibiting excellent spectral overlap with many f−f transitions in up-converting lanthanide ions, including Er^{3+}.[16,17] In such systems, Yb^{3+} acts as a sensitizer, directly absorbing externally sourced infrared input prior to energy transfer to Er^{3+}—whose subsequent radiative decay results in visible wavelength emission. Because of the highly effective RET process involved, this dual ion system typically exceeds the frequency conversion efficiency of comparable single ion, Er^{3+}-doped materials. In comparison, passive systems influence up-conversion mechanisms with ancillary components that are transparent to the optical input—participating in the UC process as providers of local field enhancement, or multibody

bridges for the transfer of energy between primary chromophores. The most familiar examples of field modification relate to plasmon-enhanced up-conversion.[18−20] However, such systems typically utilize precious metal surfaces and nanostructures, generally precluding up-conversion uses in, for example, in vivo biological labeling or imaging. The alternative, discussed within this article, considers passive mechanisms involving direct mediation with secondary chromophores codoped within the host structure. To our knowledge such research has yet to be considered within the field of up-conversion, although similar mechanisms have previously been discussed in the context of mediated RET, which characterizes the transfer of energy between donor and acceptor units through a third body.[21−23]

Here, a detailed investigation initially addresses a system in which two potentially identical donors are promoted to an electronic excited state, following interaction with an externally sourced optical input. Developing the essential principle of two-center UC (in which the acquired energy of one chromophore is transferred to the second via RET) a fully quantized representation of the local electrodynamics provides a rigorous basis for describing the result of including an additional mediator species—a neighboring, nonabsorbing chromophore. From the resulting equations, numerical models are established, based upon experimentally practicable, rare-earth ion doped, crystal lattice media. Recognizing that up-conversion optical properties in such materials are highly dependent on the physical structure, size and phase of the host, we specifically investigate how the latter—assessed by means of modeling both cubic and hexagonal lattice systems—affects UC efficiency. The investigation is then extended to assess the role of ancillary, nonresonant dopants in influencing an alternative up-conversion mechanism involving three ionic centers (where the combined energy of two active centers is transferred to a third). Subsequent analysis characterizes how mediator chromophores influence this three-center system, highlighting principles and parameters that could optimize the associated device efficiency.

■ THEORETICAL METHODS

All atomic-level electromagnetic components of the system are developed within the fully quantized framework of quantum electrodynamics (QED).[24,25] Here, the rate, Γ_{FI} of any photophysical process proceeding from any initial system state I to a final state F, is determined from the "Fermi Golden Rule"[26]

$$\Gamma_{FI} = 2\pi\hbar^{-1}\rho_f |M_{FI}|^2 \tag{1}$$

in which ρ_f represents the density of final system states. The coupling strength, between I and F is characterized by the matrix element M_{FI} formally cast, using time-dependent perturbation theory, as an infinite series, expressible in the following form:

$$M_{FI} = \sum_{q=1}^{\infty} \langle F|H_{int}(\xi)(T_0 H_{int}(\xi))^{q-1}|I\rangle \tag{2}$$

In the above expression, $T_0 \approx (E^I - H_0)^{-1}$, with E^I being the initial system energy and H_0 representing the unperturbed system Hamiltonian. The parameter q, denotes the power of the interaction Hamiltonian, $H_{int}(\xi)$, that features in each term of the expansion, this operator being defined as

$$H_{int}(\xi) = -\varepsilon_0^{-1} \sum_{\xi} \boldsymbol{\mu}(\xi) \cdot \mathbf{d}^{\perp}(\mathbf{R}_{\xi}) \tag{3}$$

where $\boldsymbol{\mu}(\xi)$ represents an electric dipole operator coupled to the transverse electric field operator $\mathbf{d}^{\perp}(\mathbf{R}_{\xi})$ at position vector $\mathbf{R}_{\xi}$. The system matter states are therefore operated on by $\boldsymbol{\mu}(\xi)$ exclusively; i.e., the ideal dipole approximation has been employed throughout. Although such methodology remains commonplace in treatments of optical frequency conversion,[27−29] it is recognized that the corresponding selection rules in rare-earth materials are to some extent compromised by spin−orbit interactions, meaning that the contribution of higher-order electric (and possibly magnetic) transitions might become significant. While not addressed further in the current study, the inclusion of such higher-order transition components can, if required, be accommodated within a multipolar expansion of the interaction Hamiltonian.[25,30] In their implementation, $\mathbf{d}^{\perp}(\mathbf{R}_{\xi})$ and $\boldsymbol{\mu}(\xi)$, respectively operate on the system radiation and matter states, the former operator expressible in general form as

$$\mathbf{d}^{\perp}(\mathbf{R}_{\xi}) = i \sum_{\mathbf{k},\eta} \left(\frac{\hbar c k \varepsilon_0}{2V}\right)^{1/2} [e^{(\eta)}(\mathbf{k})a^{(\eta)}(\mathbf{k})\exp(i\mathbf{k}\cdot\mathbf{R}_{\xi})$$
$$- \overline{e}^{(\eta)}(\mathbf{k})a^{\dagger(\eta)}(\mathbf{k})\exp(-i\mathbf{k}\cdot\mathbf{R}_{\xi})] \tag{4}$$

Equation 4 introduces familiar annihilation and creation operators, $a^{(\eta)}(\mathbf{k})$ and $a^{\dagger(\eta)}(\mathbf{k})$ that respectively modify the number of photons, of wave-vector k and polarization η, within arbitrary quantization volume V. As an inherent result of the photon creation and annihilation operators present in $H_{int}(\xi)$, the parameter q that features in eq 2 has significant physical meaning, its value corresponding to the number of fundamental matter−radiation interactions associated with a given process.

As a basis for the more complex case to follow, we first consider a system comprising two identical active centers or chromophores, a sensitizer and an activating ion, arbitrarily labeled A and A' respectively. Overall, the UC process is characterized by the initial system state $|I\rangle = |A^1 A'^1; 0(\mathbf{k},\eta)\rangle$, and final state $|F\rangle = |A^0 A'^2; 0(\mathbf{k},\eta)\rangle$. The first and second electronic excited states for the chromophore species are therefore correspondingly defined as A^1 and A^2, while the electronic ground state is labeled as A^0. The electronic levels of A and A' are assumed to be positioned (in terms of energy) in a manner that facilitates UC and proceeds though a mechanism referred to as *cross-relaxation up-conversion*, illustrated by Figure 1.

As the transfer of energy between two centers occurs via virtual photon coupling, with no net change in the number of electromagnetic field quanta, only even powers of the interaction Hamiltonian participate; i.e., only even values of q in eq 2 are considered. The leading, most significant contribution accounting for the two-center up-conversion transition is therefore second-order, and accommodates a sum over two possible intermediate system states $|R_1\rangle = |A^0 A'^1; 1(\mathbf{k},\eta)\rangle$ and $|R_2\rangle = |A^1 A'^2; 1(\mathbf{k},\eta)\rangle$. The UC mechanism develops through $|R_1\rangle$ if virtual photon creation occurs at A, with subsequent annihilation at A', while progression through $|R_2\rangle$ represents the opposite, also allowed as a result of quantum uncertainty. Accounting for both possible intermediate states, the matrix element for two-center up-conversion follows as

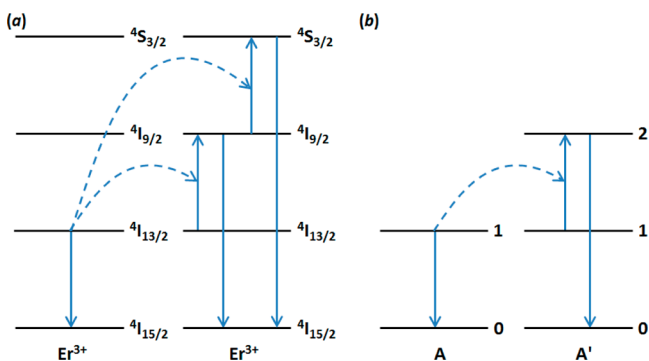$$M_{FI}^{(AA')} = \mu_i^{01(A)}\mu_j^{21(A')}V_{ij}(k, \mathbf{R}_{AA'}) \tag{5}$$

Figure 1. (a) Energy levels associated with cross-relaxation up-conversion between two Er^{3+} ions. (b) Simplified three-level representation utilized in the discussion of two-center up-conversion. Dotted line arrows represent energy transfer via RET. Higher electronic states and all vibrational levels are excluded for clarity.

The superscripts for the matrix element identify the chromophores involved in the process, and summation over repeated Cartesian indices is implied. By convention, superscript labels associated with the electronic dipole moments read from right to left, implementing the general notation $\mu^{fi(\xi)} = \langle \xi^f | \boldsymbol{\mu} | \xi^i \rangle$. Equation 5 features the fully retarded, second-rank dipole–dipole coupling tensor $V_{ij}(k, \mathbf{R}_{AA'})$,[31−33] cast in terms of the interchromophore displacement R in the following expression:

$$V_{ij}(k, \mathbf{R}) = \frac{\exp(ikR)}{4\pi\varepsilon_0 R^3}[(1 - ikR)(\delta_{ij} - 3\hat{R}_i\hat{R}_j)$$
$$- k^2R^2(\delta_{ij} - \hat{R}_i\hat{R}_j)] \tag{6}$$

As previously established, the square modulus of $M_{FI}^{(AA')}$ is required to determine the UC rate and as a means to keep the presented results general and not otherwise restricted to the description of fixed and/or highly ordered systems, chromophores are assumed at all times to be randomly orientated in three dimensions, thus

$$\langle |M_{FI}^{(AA')}|^2 \rangle = \langle \mu_i^{01(A)}\bar{\mu}_k^{01(A)}\rangle \langle \mu_j^{21(A')}\bar{\mu}_l^{21(A')}\rangle$$
$$\times \langle V_{ij}(k, \mathbf{R}_{AA'})\bar{V}_{kl}(k, \mathbf{R}_{AA'})\rangle \tag{7}$$

where angular brackets denote the required operation of a rotational average. An integration-free procedure based on isotropic matrix elements is subsequently utilized,[34,35] eq 7 requiring both second- and fourth-rank tensor averages, the former presented in the following general form:

$$\langle l_{i\lambda}l_{j\mu}\rangle = \frac{1}{3}\delta_{ij}\delta_{\lambda\mu} \tag{8}$$

in which $\langle l_{i\lambda}l_{j\mu}\rangle$ represents a product of direction cosines. Here, for example, $l_{i\lambda}$ is the cosine of the angle between the space-fixed axis i and the molecule-fixed axis λ. The generalized form of all higher-rank averages are typically presented as matrix equations, where for example the fourth-rank average, $\langle l_{i\lambda}l_{j\mu}l_{k\nu}l_{l\sigma}\rangle$ is

$$\langle l_{i\lambda}l_{j\mu}l_{k\nu}l_{l\sigma}\rangle = \frac{1}{30}\begin{pmatrix}\delta_{ij}\delta_{kl}\\\delta_{ik}\delta_{jl}\\\delta_{il}\delta_{jk}\end{pmatrix}^T\begin{pmatrix}4 & -1 & -1\\-1 & 4 & -1\\-1 & -1 & 4\end{pmatrix}\begin{pmatrix}\delta_{\lambda\mu}\delta_{\nu\sigma}\\\delta_{\lambda\nu}\delta_{\mu\sigma}\\\delta_{\lambda\sigma}\delta_{\mu\nu}\end{pmatrix} \tag{9}$$

Subsequently, using eq 8 to resolve the matter terms in eq 7 determines that

$$\langle \mu_i^{01(A)}\bar{\mu}_k^{01(A)}\rangle = \frac{1}{3}\delta_{ik}|\mu^{01(A)}|^2 \tag{10}$$

and:

$$\langle \mu_j^{21(A')}\bar{\mu}_l^{21(A')}\rangle = \frac{1}{3}\delta_{ij}|\mu^{21(A')}|^2 \tag{11}$$

while fourth-rank averaging of the associated radiation terms yields results of the form:

$$\langle V_{ij}(k, \mathbf{R})\bar{V}_{kl}(k, \mathbf{R})\rangle = \frac{1}{30}[\delta_{ij}\delta_{kl}(4V_{\lambda\lambda}(k, \mathbf{R})\bar{V}_{\mu\mu}(k, \mathbf{R})$$
$$- 2V_{\lambda\mu}(k, \mathbf{R})\bar{V}_{\lambda\mu}(k, \mathbf{R})) + (\delta_{ik}\delta_{jl} + \delta_{il}\delta_{jk})$$
$$\times (-V_{\lambda\lambda}(k, \mathbf{R})\bar{V}_{\mu\mu}(k, \mathbf{R}) + 3V_{\lambda\mu}(k, \mathbf{R})\bar{V}_{\lambda\mu}(k, \mathbf{R}))] \tag{12}$$

the above expression being dependent on both diagonal and off-diagonal representations of the coupling tensor featuring in eq 6. It is worth highlighting that the diagonal coupling tensor contributions, e.g. terms involving $V_{\lambda\lambda}$ and $\bar{V}_{\mu\mu}$ in the current example, vanish upon multiplication of eqs 10, 11 and 12, as required by eq 7. Hence, by use of the following expression:

$$V_{\lambda\mu}(k, \mathbf{R})\bar{V}_{\lambda\mu}(k, \mathbf{R}) = \frac{2}{(4\pi\varepsilon_0 R^3)^2}[(3 + k^2R^2 + k^4R^4)] \tag{13}$$

the following result is determined:

$$\langle |M_{FI}^{(AA')}|^2 \rangle = \frac{|\mu^{01(A)}|^2|\mu^{21(A')}|^2}{8(3\pi\varepsilon_0 R_{AA'}^3)^2}(3 + k^2R_{AA'}^2 + k^4R_{AA'}^4) \tag{14}$$

To entertain further mechanistic modifications that can arise through electrodynamic coupling with a third chromophore, the matrix element for up-conversion is duly modified to the following sum of four terms:

$$M_{FI} = M_{FI}^{(AA')} + M_{FI}^{(MAA')} + M_{FI}^{(AA'M)} + M_{FI}^{(AMA')} \tag{15}$$

The three-center contributions to the overall matrix element, $M_{FI}^{(MAA')}$, $M_{FI}^{(AA'M)}$, and $M_{FI}^{(AMA')}$, successively represent configurations in which a mediator chromophore, M, interacts only with A, only with A', or with both A and A' respectively. Systems featuring $M_{FI}^{(MAA')}$ and $M_{FI}^{(AA'M)}$ engage a static dipole in the mediator M, while $M_{FI}^{(AMA')}$ is dependent on the molecular polarizability of M. It is worth emphasizing again that M is specifically chosen to be essentially transparent to the optical input utilized in the initial excitation of A and A'. While calculations based on the inclusion of a single ancillary chromophore introduce the concept, and afford a basis for deriving the corresponding form of matrix element correction terms, the measurable effect in any real system has to accommodate the prospect of more than one chromophore near the active chromophores A and A' (or more generally, in the vicinity of all species actively involved in the up-conversion process). Accounting for such possibilities is not simply a matter of scaling by concentration. First, ancillary species positioned and oriented differently with respect to the active components will generate contributions of different magnitude: second, with any reasonably significant density of ancillary

species the possibility arises of quantum interference between quantum pathways involving different chromophores individually acting in the capacity of M. These interference terms can be expected to make important contributions to up-conversion rates. The matrix element for locally modified up-conversion requires the square modulus of eq 15, reducing to

$$|M_{FI}|^2 = |M_{FI}^{(AA')}|^2 + |M_{FI}^{(AMA')}|^2 + 2\text{Re}\{M_{FI}^{(AA')}\overline{M}_{FI}^{(AMA')}\} \quad (16)$$

under the assumption that the mediator will commonly represent a nonpolar chromophore. Evaluating the complete result requires $M_{FI}^{(AMA')}$, derived from fourth-order ($q = 4$) perturbation theory as

$$M_{FI}^{(AMA')} = \mu_i^{01(A)}\alpha_{jk}^{mm(M)}(-k, k)\mu_l^{21(A')}V_{ij}(k, R_{AM})$$
$$\times V_{kl}(k, R_{MA'}) \quad (17)$$

accommodating dynamic transitions in M to and from a specific state m. It is worth noting that the matrix element presented as eq 17 is similar in form to that utilized in the discussion of third body mediated RET, although the latter necessarily engages different electronic levels of the associated donor and acceptor chromophores.[21−23] The second-rank dispersion polarizability tensor $\alpha_{jk}^{mm(M)}(-k,k)$ has been utilized, a general representation of which is

$$\alpha_{ij}^{nm(\xi)}(-k_1; k_2) = \sum_r \left(\frac{\mu_j^{nr(\xi)}\mu_i^{rm(\xi)}}{E^{rm(\xi)} - \hbar ck_2} + \frac{\mu_i^{nr(\xi)}\mu_j^{rm(\xi)}}{E^{rm(\xi)} + \hbar ck_1} \right) \quad (18)$$

using shorthand notation to describe state energy differences, for example $E^{rm(\xi)} = E^{r(\xi)} - E^{m(\xi)}$. The second term on the right in eq 16 is therefore given by the modulus square of eq 17, which is presented in the following form:

$$\langle |M_{FI}^{(AMA')}|^2 \rangle = \langle \mu_i^{01(A)}\overline{\mu}_m^{01(A)} \rangle \langle \mu_l^{21(A')}\overline{\mu}_p^{21(A')} \rangle$$
$$\times \langle \alpha_{jk}^{mm(M)}(-k, k)\overline{\alpha}_{no}^{mm(M)}(-k, k) \rangle$$
$$\times \langle V_{ij}(k, R_{AM})\overline{V}_{mn}(k, R_{AM}) \rangle \langle V_{kl}(k, R_{MA'})\overline{V}_{op}(k, R_{MA'}) \rangle \quad (19)$$

Using both the second- and fourth-rank equations established previously, the rotationally averaged result is

$$\langle |M_{FI}^{(AMA')}|^2 \rangle = \frac{|\mu^{01(A)}|^2|\mu^{21(A')}|^2|\alpha^{mm(M)}|^2}{64(3\pi\varepsilon_0)^4 R_{AM}{}^6 R_{MA'}{}^6}$$
$$\times (9 + 3k^2 R_{AM}{}^2 + 3k^2 R_{MA'}{}^2 + 3k^4 R_{AM}{}^4 + 3k^4 R_{MA'}{}^4$$
$$+ k^4 R_{AM}{}^2 R_{MA'}{}^2 + k^6 R_{AM}{}^4 R_{MA'}{}^2 + k^6 R_{AM}{}^2 R_{MA'}{}^4$$
$$+ k^8 R_{AM}{}^4 R_{MA'}{}^4) \quad (20)$$

The remaining contribution to the locally modified UC matrix element—the last term on the right in eq 16 − represents a quantum inference, being the cross product of the two- and three-center matrix elements $M_{FI}^{(AA')}$ and $\overline{M}_{FI}^{(AMA')}$. Combining eqs 5 and 17, this cross-term is represented as

$$\langle M_{FI}^{(AA')}\overline{M}_{FI}^{(AMA')} \rangle = \langle \mu_i^{01(A)}\overline{\mu}_i^{01(A)} \rangle \langle \mu_j^{21(A')}\overline{\mu}_l^{21(A')} \rangle$$
$$\times \langle \overline{\alpha}_{jk}^{mm(M)}(-k, k) \rangle \langle V_{ij}(k, R_{AA'}) \rangle \langle \overline{V}_{ij}(k, R_{AM}) \rangle$$
$$\times \langle \overline{V}_{kl}(k, R_{MA'}) \rangle \quad (21)$$

and the overall contribution to locally modified up-conversion attributed by the quantum cross-term is subsequently derived as

$$\langle M_{FI}^{(AA')}\overline{M}_{FI}^{(AMA')} \rangle$$
$$= -\frac{|\mu^{01(A)}|^2|\mu^{21(A')}|^2\overline{\alpha}_{\lambda\lambda}^{mm(M)}k^6 \exp(ik(R_{AA'} - R_{AM} - R_{MA'}))}{72(3\pi\varepsilon_0)^3 R_{AA'} R_{AM} R_{MA'}} \quad (22)$$

where $\overline{\alpha}_{\lambda\lambda}^{mm(M)}$ denotes the scalar trace of the polarizability tensor. The complete two-center UC matrix element is therefore expressible as a sum of the results from eqs 14, 20, and 22. These expressions for two- and three-center UC, vary with approximately R^{-6}, R^{-12} and R^{-3} dependences, respectively (ignoring, for this purpose, the distinction between $R_{AA'}$, R_{AM} and $R_{MA'}$). As a cross-term between the $|M_{FI}^{(AA')}|^2$ and $|M_{FI}^{(AMA')}|^2$ contributions, it might have been expected that $M_{FI}^{(AA')} \overline{M}_{FI}^{(AMA')}$ would vary with R^{-9} rather than the discovered R^{-3} relationship: however, in comparison to eqs 7 and 19, the orientational average of the quantum cross-term uniquely features second-rank averages of the intermolecular coupling tensor. Focusing on one example, the result of $\langle V_{ij}(k, \mathbf{R}_{AA'}) \rangle$ in eq 21 is

$$\langle V_{ij}(k, \mathbf{R}_{AA'}) \rangle = \frac{1}{3}\delta_{ij}V_{\lambda\lambda}(k, \mathbf{R}_{AA'}) \quad (23)$$

highlighting a dependence on the pure diagonal components of the second-rank tensor—noting again that until now, such components have always vanished as a result of isotropic averaging. Continuing with the current example, $V_{\lambda\lambda}(k, \mathbf{R})$ is expressible as

$$V_{\lambda\lambda}(k, \mathbf{R}) = -\frac{\exp(ikR)}{2\pi\varepsilon_0 R^3}[k^2 R^2] \quad (24)$$

which by contrast to the complete dipole–dipole coupling tensor, eq 6, features no short- and midrange terms (those which have higher inverse power dependencies on each chromophore separation). The averaged results therefore determine in principle that the magnitude of the three-center mechanism characterized by $|M_{FI}^{(AMA')}|^2$ will dominate at small interchromophore distances, while the $M_{FI}^{(AA')}\overline{M}_{FI}^{(AMA')}$ contribution will become more prominent at larger separations. Such predictions are now tested by the development of numerical models, whose parameters are selected to accurately reflect the conditions within lanthanide doped crystal systems.

■ RESULTS AND DISCUSSION

Fluoride-based crystalline materials such as $NaYF_4$ or more generally $Na(RE)F_4$ (RE representing any commonly utilized rare-earth ion such as Yb^{3+} or Er^{3+}) are commonly utilized as structures to incorporate lanthanide ion up-conversion systems. Such media are known to exhibit low phonon energies and compatible lattice dimensions with respect to dopant ion size, the former resulting in limited competing, nonradiative energy losses, while the latter contributes to high structural stability of the host. Specific properties of $Na(RE)F_4$, such as crystal size and phase depend on reaction temperature, dopant concentration and other experimental parameters utilized in their synthesis, such sensitivity having been exploited by a number of research groups exploring the fabrication of designer optical materials with tunable optical properties.[36−41] Typically, $Na(RE)F_4$ crystals exist in one of two forms, being either

23538

dx.doi.org/10.1021/jp507262a | J. Phys. Chem. C 2014, 118, 23535−23544

cubic or hexagonal phase, the latter in the case of Yb/Er doped NaYF$_4$ exhibiting an order of magnitude UC efficiency improvement with respect to the cubic counterpart.[10,42] While such phase-dependent optical properties can be characterized in terms of crystal field strengths around the dopant ions, eqs 14, 20, and 22 suggest that locally modified up-conversion is highly dependent on interchromophore separation, a factor that is also inherently phase dependent. The influence of a third-component mediator, locally modifying the rate of up-conversion within crystal media, is now assessed by a numerical method comparing the magnitude of the derived two- and three-center up-conversion expressions. Focusing on the variable relative positioning of ancillary dopants relative to the UC pair, three distinct crystal structures are considered: simple-cubic, simple-hexagonal and hexagonal close-packed, beginning with assessment of the former.

A notional cubic lattice is considered, the crystalline host modeled by placement of chromophores on sites within cells on a $5 \times 5 \times 5$ three-dimensional structure, illustrated in Figure 2. The key optical and electronic parameters are set with $\mu^{01(A)}$
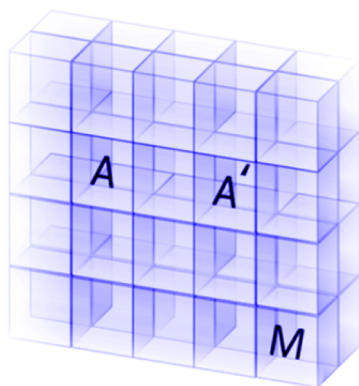

Figure 2. Part of the three-dimensional cell structure used for simulations of three-component up-conversion.

$= \mu^{21(A')} = 5.00 \times 10^{-31}$ C m, $\alpha_{\lambda\lambda}^{mm(M)} = 2.00 \times 10^{-39}$ J^{-1} C^2 m^2, and $k = 6.4 \times 10^6$ m^{-1} — the latter signifying an infrared optical input. Interchromophore separations are expressed as $R_{\xi_1\xi_2} = m_{\xi_1\xi_2}a$, with a, and $m_{\xi_1\xi_2}$ respectively denoting the lattice constant and the separation between ξ_1 and ξ_2 in terms of unit spaces. The sites occupied by A and A' are located at fixed positions on the middle row of the middle layer of the cube with $R_{AA'} = 2a$ — the double spacing providing for a consideration of cases where the ancillary dopant may be located between the two active ions. With no other A species present within the system, this establishes a primary chromophore concentration of approximately 2 mol %. Any number of individual M chromophores can be assigned to other unit spaces in the lattice available for occupancy (the number determined by the level of doping to be modeled), and results are determined such that the combined three-center UC magnitude for the system is the sum of all individual contributions.

As previously discussed, a significant influence on the overall effect of mediator interaction on the rate of up-conversion is the relative separation of the primary and ancillary chromophores. The effect of interchromophore distance on the rate of up-conversion can therefore be systematically investigated by varying the lattice constant: the results are presented in Figure 3.
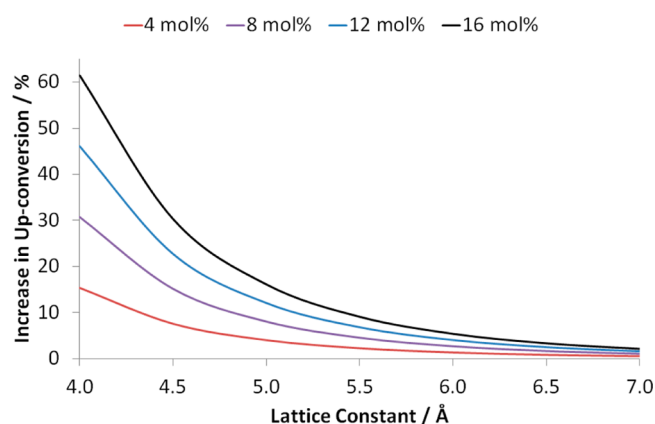

Figure 3. Predicted improvements in up-conversion efficiency as a result of mediator codoping. The four data series represent secondary chromophore concentrations within the modeled lattice.

Clearly, strikingly large enhancements can be achieved under suitable conditions. Even for a modest 16 mol % secondary chromophore concentration, and a lattice constant of 5.5 Å, an overall efficiency increase of approximately 10% is determined. To put this into context, for cubic phase NaYF$_4$ (with a reported lattice constant of 5.5 Å),[43] codoped Yb^{3+} and Er^{3+} systems—although an example of active UC—are reported to be most efficient at 2 mol % and approximately 20 mol % concentrations, respectively.[16,17]

The ancillary dopants that contribute most to the locally modified up-conversion efficiency, are those located at lattice sites directly adjacent to the sensitizer and/or the activating ion. Focusing on the nearest neighbor environment of each such center individually, primary ions in a simple cubic arrangement are surrounded by a maximum number of six secondary chromophores (four in the arbitrarily assigned x,y-plane, one directly above and one directly below in the z-axis). By comparison, as illustrated by Figure 4, any activating ion in a simple hexagonal system has the potential to be surrounded by eight ancillary dopants (six in the x,y-plane, and two in the sites directly above and below). A rise in the maximum number of closest neighbor secondary chromophores is expected to increase the magnitude of locally modified up-conversion, suggesting that the rate of UC is enhanced within a hexagonal crystal structure, relative to a cubic counterpart.

It is important to also consider the effect of modifying the lattice constant, c which determines the z-axis separation of the crystal layers, where $c = a$ for the previously considered simple cubic system. Although lattice parameters may vary with the experimental conditions used to fabricate the structure, for Na(RE)F$_4$ crystals, c is typically less than a, e.g., for NaYF$_4$, $a = 5.96$ Å and $c = 3.53$ Å.[38] Such conditions suggest that the most significant contributions to the three-center UC rate are attributed to secondary chromophores located in directly neighboring sites of adjacent layers to the primary molecular centers. In evaluating hexagonal lattice systems, both simple and close-packed structures are considered beginning with the former.

Assuming the numerical value of key electronic parameters $\mu^{01(A)}$, $\mu^{21(A')}$, $\alpha_{\lambda\lambda}^{mm(M)}$, and k remain unchanged, only the geometric position of the lattice sites relative to each other has
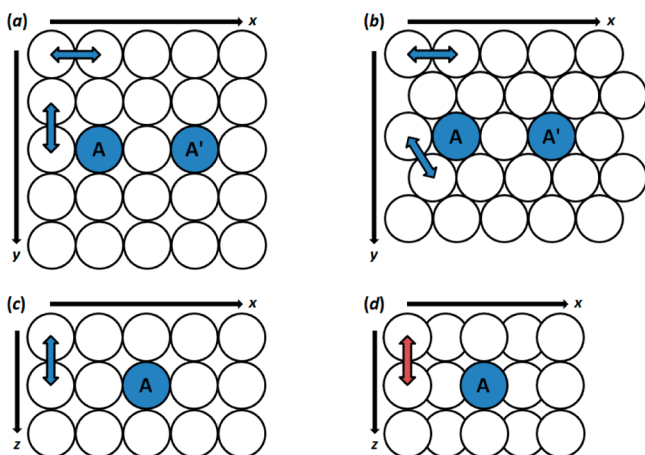
Figure 4. Pictorial representations of simple cubic and simple hexagonal lattice structures. (a and b) Entire middle layer projected in the x,y-plane of the cubic and hexagonal systems, respectively. (c and d) Correspondingly, a cross-sectional view of the middle three layers of both the cubic and hexagonal systems in the x,z-plane. Blue and red double headed arrows indicate a separation of lattice sites by constants a and c, respectively.

to be reconsidered in order to directly evaluate UC rates within simple hexagonal-phase structures. The modified numerical model consists of five layers, as illustrated in Figure 4b, with each positioned directly above the last—the lattice constant c is introduced to accommodate the separation between layers. As before, the primary chromophores are located at fixed positions on the middle row of the middle layer with $R_{AA'} = 2a$. Figure 5
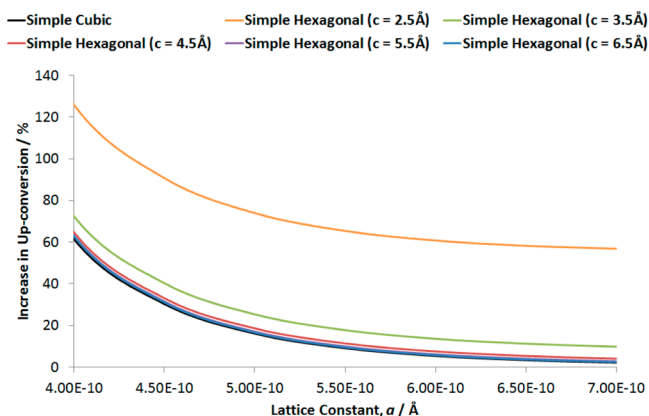

Figure 5. Predicted improvements in up-conversion efficiency as a result of mediator codoping in both simple cubic and hexagonal systems.

shows the result of varying both a and c for the hexagonal system under fixed 16 mol % secondary chromophore concentration. Equivalent results for the simple cubic system are also represented in order to allow direct comparison between the two systems.

Although generally higher in all instances, the predicted increase in up-conversion for a simple hexagonal system relative to a cubic counterpart becomes significant only for small values of c—less than 3.5 Å for the current model. Indeed, establishing realistic dimensions of a = 6.0 Å and c = 3.5 Å, directly neighboring sites of the primary chromophores in adjacent layers, i.e., those immediately above or below the middle layer, attribute the most significant contribution to three-center UC,

second only to the single lattice site located directly between A and A′. Although relatively simple to model, it is recognized that simple or primitive lattice structures (cubic or hexagonal), are generally rare and that more efficient, close-packed systems are more prevalent.

A hexagonal close-packed structure is essentially identical to the previously regarded primitive arrangement with the provision that alternating layers of the host are positioned to fill the gaps formed between neighboring lattice sites of adjacent layers, consequently establishing a repeating A−B−A−B type structure as illustrated by Figure 6. It is worth
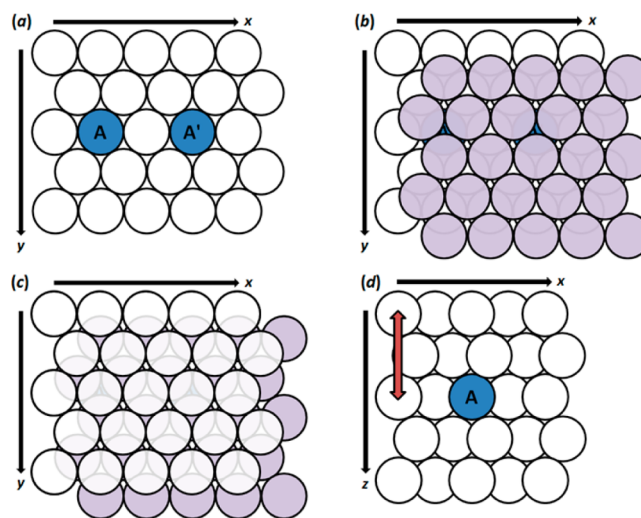

Figure 6. Pictorial representation of a close-packed hexagonal lattice structure. (a−c) Sequential construction of the top three layers (the color change of lattice sites is used only for clarity of illustration). (d) Cross-sectional view of the entire structure.

highlighting at this point that the closely related cubic close-packed, i.e., the A−B−C−A−B−C layered structure is not presently considered in detail. Such a system is likely to deliver an identical result to the current hexagonal close-packed arrangement on the grounds of identical inherent symmetry.

The lattice constant c determines the distance between adjacent, spatially overlapping layers, as shown in Figure 6d. By virtue of the adopted close-packed arrangement, secondary chromophores in such an arrangement will on average be positioned in closer proximity to the primary UC molecular centers, the predicted increase in UC is duly presented as Figure 7.

Similar to the previous comparison of simple cubic and hexagonal structures, a trend is established whereby a close-packed hexagonal system relative to a primitive counterpart exhibits larger increases in UC across all equivalently modeled lattice constants. Comparison of the two contour graphs in Figure 7 however illustrates that recorded increases in up-conversion as both a and c decrease, occur much more rapidly in the close-packed system, further highlighting the significant sensitivity over the short-range regime of the mediated or three-center UC.

The current up-conversion mechanism based upon cross-relaxation imposes a condition that the active chromophores have suitably positioned higher electronic states, to accommodate the energy released as a result of lower level relaxation; i.e., it is assumed that an accessible excited state A^2 is located at twice the relative energy of the A^1 level. Greater flexibility in
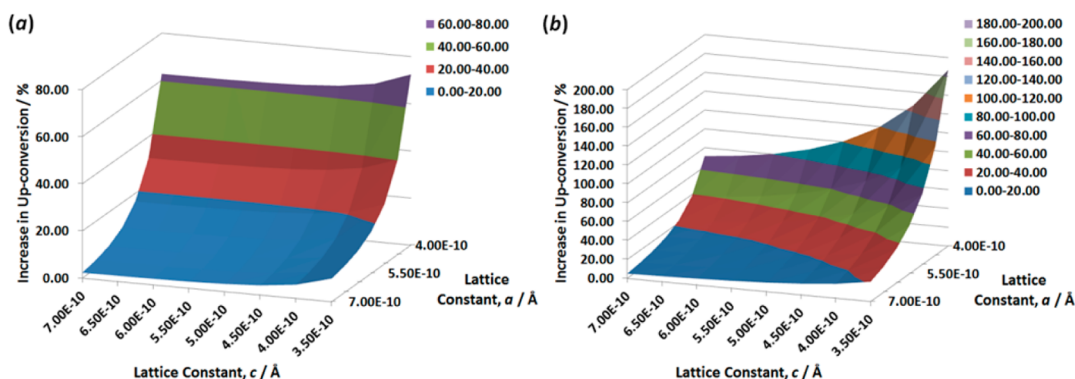
Figure 7. Comparison of predicted up-conversion improvements for simple and close-packed hexagonal systems presented as parts a and b, respectively. A fixed 16 mol % ancillary dopant concentration is utilized for both systems.
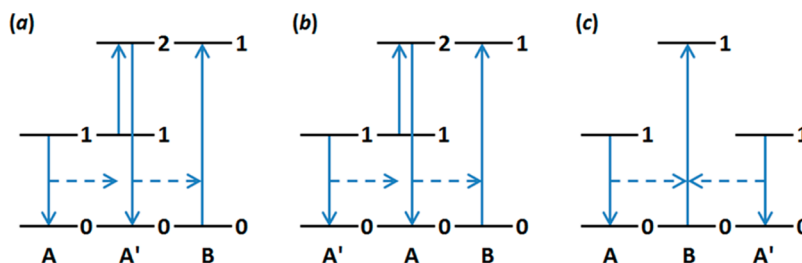

Figure 8. Electronic state, energy level representations of accretive and co-operative three-center up-conversion. The former is characterized by both the AA′B and A′AB configurations, portrayed by diagrams a and b, respectively. Diagram c illustrates the ABA′ configuration in which the activating ion interacts directly with both sensitizers.

tailoring the optical response is afforded by relaxing the constraint that the sensitizer and activating ions are identical. The model presented in this report is readily extensible in this respect, for example, to account for two identical sensitizers transferring energy to a single activating ion, selected to accommodate the combined sensitizer energy—representative energy level diagrams are presented as Figure 8.

The matrix element for three-center up-conversion is presented as follows:

$$M_{FI} = M_{FI}^{(AA'B)} + M_{FI}^{(A'AB)} + M_{FI}^{(ABA')} \qquad (25)$$

noting redefinition of the activating ion as B. The first two terms of eq 25 describe a form of accretive up-conversion in which the activating ion essentially receives the combined energy acquired by both A and A′ through interaction with only one of the two sensitizers.[44] Both mechanisms therefore inherently feature a process of cross-relaxation UC as previously outlined. We therefore focus on the cooperative process, portrayed by Figure 8c, in which A and A′ both interact with B. Developed from fourth-order perturbation theory, this mechanism, defined by $M_{FI}^{(ABA')}$ is analogous in form to eq 17, with a rotationally averaged result that is identical to eq 20 upon substitution of $\mu^{21(A')}$ with $\mu^{01(A')}$, $\alpha^{mm(M)}$ with $\alpha^{01(B)}$, and with all references to the mediator M substituted to refer to the activating ion B, so that for example R_{AM} becomes R_{AB}.

The influence on co-operative, three-center up-conversion by an ancillary chromophore is now considered. Under the continued assumption that the mediator represents a nonpolar chromophore, the matrix element for the overall mechanism reduces to a sum of three distinct terms:

$$M_{FI} = M_{FI}^{(ABA')} + M_{FI}^{(AMBA')} + M_{FI}^{(ABMA')} \qquad (26)$$

Utilizing established theory, the rate of locally modified, cooperative up-conversion requires the square modulus of eq 26, delivered as

$$|M_{FI}|^2 = |M_{FI}^{(ABA')}|^2 + |M_{FI}^{(ABMA')}|^2 + |M_{FI}^{(AMBA')}|^2$$
$$+ 2\text{Re}\{M_{FI}^{(ABA')}M_{FI}^{(AMBA')} + M_{FI}^{(ABA')}M_{FI}^{(ABMA')}$$
$$+ M_{FI}^{(AMBA')}M_{FI}^{(ABMA')}\} \qquad (27)$$

in which the last three terms of eq 27 again represent contributions associated with quantum interference. As previously determined in the example of locally modified two-center up-conversion, such correction terms represent relatively marginal contributions to the overall up-conversion mechanism, at least in the range of intermolecular separations consistent with rare-earth doped crystal lattice media. The remaining terms in eq 27 require the matrix elements $M_{FI}^{(ABMA')}$ and $M_{FI}^{(AMBA')}$ derived from sixth-order perturbation theory. Subsequently the rate of locally modified, three-center UC is determined as the sum of $|M_{FI}^{(ABMA')}|^2$ and $|M_{FI}^{(AMBA')}|^2$:

$$\langle|M_{FI}^{(ABMA')}|^2\rangle + \langle|M_{FI}^{(AMBA')}|^2\rangle$$
$$= \frac{|\mu^{01(A)}|^2|\mu^{01(A')}|^2|\alpha^{mm(M)}|^2|\alpha^{10(B)}|^2}{512 \times 3^4 (\pi\varepsilon_0)^6}$$
$$\times (R_{AB}{}^{-6}R_{BM}{}^{-6}R_{MA'}{}^{-6} + R_{AM}{}^{-6}R_{MB}{}^{-6}R_{BA'}{}^{-6}) \qquad (28)$$

For clarity of presentation, eq 28 has been presented as the short-range asymptote of the complete result required to fully characterize the UC process for any specified intermolecular separation. By comparison, the short-range limit of the three-

23541

dx.doi.org/10.1021/jp507262a | J. Phys. Chem. C 2014, 118, 23535−23544

center up-conversion process, expressed previously as $|M_{FI}^{(ABA')}|^2$ is

$$\langle |M_{FI}^{(ABA')}|^2 \rangle = \frac{|\mu^{01(A)}|^2 |\mu^{01(A')}|^2 |\alpha^{10(B)}|^2}{64 \times 3^2 (\pi \varepsilon_0)^4 R_{AB}{}^6 R_{BA'}{}^6} \tag{29}$$

The overall enhancement of cross-sensitization UC by inclusion of ancillary, mediator chromophores can therefore be quantitatively assessed by comparison of eqs 28 and 29. Initial results based upon simplifying assumptions that all interchromophore separations in the two equations are equivalent, taking $\mu^{01(A)} = \mu^{01(A')} = 5.00 \times 10^{-31}$ C m and $\alpha^{mm(M)} = \alpha^{10(B)} = 2.00 \times 10^{-39}$ J^{-1} C^2 m^2, indicate that the mediator-influenced contribution to the overall process of three-center up-conversion dominates at short interchromophore separations. Specifically, a 60% increase in the rate of UC is predicted at $R = 2.5$ Å, where $R = R_{AB} = R_{BM} = R_{MA'} = R_{AM} = R_{BA'}$. By comparison, the predicted increase in the rate of UC reduces to approximately 1% as R increases up to 5.0 Å. It should however be noted that these preliminary findings only consider the influence of a single mediator located in near vicinity to the closely distributed A, A', and B chromophores. In practice, experimental conditions will likely dictate that numerous ancillary dopants interact with each set of sensitizer and acceptor ions. A sum of all such interactions will require a more detailed numerical model that remains the focus of possible future investigation.

■ CONCLUSIONS

The results of this research show that ancillary chromophore doping at positions in the vicinity of neighboring primary chromophores can significantly enhance the rate of non-parametric up-conversion as a result of passive interactions. Such improvement, achieved as a result of energy mediation through nonresonant chromophores, is most significant in the short-range regime where energy transfer between the associated molecular centers is most efficient—vindicating the use of a relatively small lattice sample space in the present numerical simulations. The concentration of doped mediators as well as the experimentally influenced lattice parameters and crystal phase of the host will all have a significant effect on the relative positioning or both primary and secondary chromophores, and therefore represent the most significant variables to evaluate in the pursuit of locally modified up-conversion.

All current data strongly suggests that ancillary chromophore interactions with primary optical centers within up-conversion systems are characterized as UC enhancement—yet in principle, it should prove possible to tailor, optical materials with reduced up-conversion efficiency. Exploiting the latter effect could prove beneficial for systems in which noncoherent up-conversion proves deleterious to an intended purpose. For example, the occurrence of UC in rare-earth fiber lasers can exact significant losses in the sought population inversion, diminishing the fundamental output.[45,46] For mediator modified two-center up-conversion, in a chromophore separation range determined by lanthanide ion-doped crystal lattices, it transpires that the quantum cross-term, $M_{FI}^{(AA')} \overline{M}_{FI}^{(AMA')}$ derived as eq 22, delivers a negative contribution to the UC rate, yet one that is marginal compared to the magnitude of the terms arising from the mechanisms associated with $|M_{FI}^{(AA')}|^2$ and $|M_{FI}^{(AMA')}|^2$ — at least in materials incorporating isotropically arranged optical centers. Similar results, although

currently unverified through robust numerical modeling, are predicted with regards to the quantum interference terms associated with locally modified three-center up-conversion. In principle, however, this study suggests that materials will inhibit up-conversion if their design allows the quantum cross-terms to dominate the up-conversion. Identifying the means to achieve such an effect may prove possible through modeling of more specialized, ordered systems[47] — such a situation may also exploit the use of weighted rotational averaging.[48] The sign of the ancillary dopant polarizability, as determined by the relative positioning of initial and intermediate state electronic levels relative to the optical input, may also prove significant in achieving suppressed or indeed, further enhanced UC efficiency.

Our current system does not account for the dynamics of the system in terms of its temporal evolution, since the most obvious range of potential applications are those leading to steady output from sample material. As a prospect representing scope for future work, however, it might be interesting to reflect on the possible effects of reducing the scale of these up-conversion materials to the nanoscale, where for example it has been found that a reduction in particle size provides the ability to modify the lifetime of intermediate states.[13] Also, crystal phase is only currently considered by its role in modifying interchromophore distances, and not for example by geometric symmetry effects that may play a significant role in modifying local crystal field symmetry. It is well established that crystal lattice structures that exhibit low levels of symmetry around the primary optical centers exhibit heightened UC efficiency as such systems permit greater intermixing of the lanthanide f-states with higher energy electronic levels—partially overcoming the strictly forbidden nature of f–f level transitions within lanthanide ions.[13,49] More sophisticated applications of the derived equations to complex types of optical media will also require account to be taken of other, possibly competing primary chromophores—it can be anticipated that the emerging result will exhibit a sensitive dependence on the ratio of these centers with the number of mediators. Current attempts to quantitate mediator effects do however show promise and warrant further investigation, leading toward test-bed calculations for systems of specific chemical constitution and crystalline habit.

■ AUTHOR INFORMATION

Corresponding Author
*(D.L.A.) E-mail: d.l.andrews@uea.ac.uk. Telephone: +441603 592014.

Notes
The authors declare no competing financial interests.

■ REFERENCES

(1) Li, C.; Yang, X.; Yu, J. C.; Ming, T.; Wang, J. Porous Upconversion Materials-Assisted Near Infrared Energy Harvesting by Chlorophylls. *Chem. Commun.* **2011**, *47*, 3511−3513.
(2) Cheng, Y. Y.; Fückel, B.; MacQueen, R. W.; Khoury, T.; Clady, R. G. C. R.; Schulze, T. F.; Ekins-Daukes, N. J.; Crossley, M. J.;

Stannowski, B.; Lips, K.; et al. Improving the Light-Harvesting of Amorphous Silicon Solar Cells with Photochemical Upconversion. *Energy Environ. Sci.* **2012**, *5*, 6953–6959.

(3) Huang, X.; Han, S.; Huang, W.; Liu, X. Enhancing Solar Cell Efficiency: The Search for Luminescent Materials as Spectral Converters. *Chem. Soc. Rev.* **2013**, *42*, 173–201.

(4) Chatterjee, D. K.; Gnanasammandhan, M. K.; Zhang, Y. Small Upconverting Fluorescent Nanoparticles for Biomedical Applications. *Small* **2010**, *6*, 2781–2795.

(5) Zhang, C.; Sun, L.; Zhang, Y.; Yan, C. Rare Earth Upconversion Nanophosphors: Synthesis, Functionalization and Application as Biolabels and Energy Transfer Donors. *J. Rare Earths* **2010**, *28*, 807–819.

(6) Chen, J.; Zhao, J. X. Upconversion Nanomaterials: Synthesis, Mechanism, and Applications in Sensing. *Sensors* **2012**, *12*, 2414–2435.

(7) Lupei, A.; Lupei, V.; Gheorghe, C.; Ikesue, A.; Osiac, E. Upconversion Emission of RE^{3+} in Sc_2O_3 Ceramic under 800 nm Pumping. *Opt. Mater.* **2009**, *31*, 744–749.

(8) Desirena, H.; De la Rosa, E.; Salas, P.; Meza, O. Red, Green, Blue and White Light Upconversion Emission in $Yb^{3+}/Tm^{3+}/Ho^{3+}$ Co-Doped Tellurite Glasses. *J. Phys. Appl. Phys.* **2011**, *44*, 455308.

(9) Xu, Y.; Wang, Y.; Shi, L.; Xing, L.; Tan, X. Bright White Upconversion Luminescence in $Ho^{3+}/Yb^{3+}/Tm^{3+}$ Triple Doped $CaWO_4$ Polycrystals. *Opt. Laser Technol.* **2013**, *54*, 50–52.

(10) Wang, F.; Liu, X. Recent Advances in the Chemistry of Lanthanide-Doped Upconversion Nanocrystals. *Chem. Soc. Rev.* **2009**, *38*, 976–989.

(11) Haase, M.; Schäfer, H. Upconverting Nanoparticles. *Angew. Chem., Int. Ed.* **2011**, *50*, 5808–5829.

(12) Dong, H.; Sun, L.-D.; Yan, C.-H. Basic Understanding of the Lanthanide Related Upconversion Emissions. *Nanoscale* **2013**, *5*, 5703–5714.

(13) Chen, G.; Yang, C.; Prasad, P. N. Nanophotonics and Nanochemistry: Controlling the Excitation Dynamics for Frequency Up- and Down-Conversion in Lanthanide-Doped Nanoparticles. *Acc. Chem. Res.* **2013**, *46*, 1474–1486.

(14) Jenkins, R. D.; Andrews, D. L. Orientation Factors in Three-Centre Energy Pooling. *Phys. Chem. Chem. Phys.* **2000**, *2*, 2837–2843.

(15) Andrews, D. L.; Jenkins, R. D. A Quantum Electrodynamical Theory of Three-Center Energy Transfer for Upconversion and Downconversion in Rare Earth Doped Materials. *J. Chem. Phys.* **2001**, *114*, 1089–1100.

(16) Suyver, J. F.; Grimm, J.; Krämer, K. W.; Güdel, H. U. Highly Efficient Near-Infrared to Visible Up-Conversion Process in $NaYF_4:Er^{3+},Yb^{3+}$. *J. Lumin.* **2005**, *114*, 53–59.

(17) Cao, B. S.; He, Y. Y.; Zhang, L.; Dong, B. Upconversion Properties of $Er^{3+}-Yb^{3+}:NaYF_4$ Phosphors with a Wide Range of Yb^{3+} Concentration. *J. Lumin.* **2013**, *135*, 128–132.

(18) Zhang, W.; Ding, F.; Chou, S. Y. Large Enhancement of Upconversion Luminescence of $NaYF_4:Yb^{3+}/Er^{3+}$ Nanocrystal by 3D Plasmonic Nano-Antennas. *Adv. Mater.* **2012**, *24*, OP236–OP241.

(19) Luu, Q.; Hor, A.; Fisher, J.; Anderson, R. B.; Liu, S.; Luk, T.-S.; Paudel, H. P.; Farrokh Baroughi, M.; May, P. S.; Smith, S. Two-Color Surface Plasmon Polariton Enhanced Upconversion in $NaYF_4:Yb:Tm$ Nanoparticles on Au Nanopillar Arrays. *J. Phys. Chem. C* **2014**, *118*, 3251–3257.

(20) Sun, Q.-C.; Mundoor, H.; Ribot, J. C.; Singh, V.; Smalyukh, I. I.; Nagpal, P. Plasmon-Enhanced Energy Transfer for Improved Upconversion of Infrared Radiation in Doped-Lanthanide Nanocrystals. *Nano Lett.* **2014**, *14*, 101–106.

(21) Daniels, G. J.; Andrews, D. L. The Electronic Influence of a Third Body on Resonance Energy Transfer. *J. Chem. Phys.* **2002**, *116*, 6701–6712.

(22) Salam, A. Mediation of Resonance Energy Transfer by a Third Molecule. *J. Chem. Phys.* **2012**, *136*, 014509.

(23) Ford, J. S.; Andrews, D. L. Resonance Energy Transfer: Influence of Neighboring Matter Absorbing in the Wavelength Region of the Acceptor. *J. Chem. Phys.* **2013**, *139*, 014107.

(24) Craig, D. P.; Thirunamachandran, T. *Molecular Quantum Electrodynamics*; Dover: New York, 1998.

(25) Salam, A. Molecular Quantum Electrodynamics in the Heisenberg Picture: A Field Theoretic Viewpoint. *Int. Rev. Phys. Chem.* **2008**, *27*, 405–448.

(26) Grynberg, G.; Aspect, A.; Fabre, C. *Introduction to Quantum Optics*; Cambridge University Press: Cambridge, U.K., 2010.

(27) Diaz-Torres, L. A.; Meza, O.; Solis, D.; Salas, P.; De la Rosa, E. Visible Upconversion Emission and Non-Radiative Direct Yb^{3+} to Er^{3+} Energy Transfer Processes in Nanocrystalline $ZrO_2:Yb^{3+},Er^{3+}$. *Opt. Lasers Eng.* **2011**, *49*, 703–708.

(28) Herter, B.; Wolf, S.; Fischer, S.; Gutmann, J.; Bläsi, B.; Goldschmidt, J. C. Increased Upconversion Quantum Yield in Photonic Structures due to Local Field Enhancement and Modification of the Local Density of States − A Simulation-Based Analysis. *Opt. Express* **2013**, *21*, A883–A900.

(29) Fujii, M.; Nakano, T.; Imakita, K.; Hayashi, S. Upconversion Luminescence of Er and Yb Codoped $NaYF_4$ Nanoparticles with Metal Shells. *J. Phys. Chem. C* **2013**, *117*, 1113–1120.

(30) Scholes, G. D.; Andrews, D. L. Damping and Higher Multipole Effects in the Quantum Electrodynamical Model for Electronic Energy Transfer in the Condensed Phase. *J. Chem. Phys.* **1997**, *107*, 5374–5384.

(31) Andrews, D. L.; Bradshaw, D. S. Virtual Photons, Dipole Fields and Energy Transfer: A Quantum Electrodynamical Approach. *Eur. J. Phys.* **2004**, *25*, 845–858.

(32) Salam, A. A General Formula for the Rate of Resonant Transfer of Energy between Two Electric Multipole Moments of Arbitrary Order Using Molecular Quantum Electrodynamics. *J. Chem. Phys.* **2005**, *122*, 044112.

(33) Dávila Romero, L. C.; Andrews, D. L. A Retarded Coupling Approach to Intermolecular Interactions. *J. Phys. B: At. Mol. Opt. Phys.* **2009**, *42*, 085403.

(34) Andrews, D. L.; Thirunamachandran, T. On Three-Dimensional Rotational Averages. *J. Chem. Phys.* **1977**, *67*, 5026–5033.

(35) Wagnière, G. The Evaluation of Three-Dimensional Rotational Averages. *J. Chem. Phys.* **1982**, *76*, 473–480.

(36) Sun, Y.; Chen, Y.; Tian, L.; Yu, Y.; Kong, X.; Zhao, J.; Zhang, H. Controlled Synthesis and Morphology Dependent Upconversion Luminescence of $NaYF_4:Yb$, Er Nanocrystals. *Nanotechnology* **2007**, *18*, 275609.

(37) Li, C.; Quan, Z.; Yang, P.; Yang, J.; Lian, H.; Lin, J. Shape Controllable Synthesis and Upconversion Properties of $NaYbF_4/NaYbF_4:Er^{3+}$ and $YbF_3/YbF_3:Er^{3+}$ Microstructures. *J. Mater. Chem.* **2008**, *18*, 1353–1361.

(38) Wang, F.; Han, Y.; Lim, C. S.; Lu, Y.; Wang, J.; Xu, J.; Chen, H.; Zhang, C.; Hong, M.; Liu, X. Simultaneous Phase and Size Control of Upconversion Nanocrystals through Lanthanide Doping. *Nature* **2010**, *463*, 1061–1065.

(39) Wang, H.; Yi, Z.; Rao, L.; Liu, H.; Zeng, S. High Quality Multi-Functional $NaErF_4$ Nanocrystals: Structure-Controlled Synthesis, Phase-Induced Multi-Color Emissions and Tunable Magnetic Properties. *J. Mater. Chem. C* **2013**, *1*, 5520–5526.

(40) Wang, J.; Song, H.; Xu, W.; Dong, B.; Xu, S.; Chen, B.; Yu, W.; Zhang, S. Phase Transition, Size Control and Color Tuning of $NaREF_4:Yb^{3+}$, Er^{3+} (RE = Y, Lu) Nanocrystals. *Nanoscale* **2013**, *5*, 3412–3420.

(41) Lin, M.; Zhao, Y.; Liu, M.; Qiu, M.; Dong, Y.; Duan, Z.; Li, Y. H.; Pingguan-Murphy, B.; Lu, T. J.; Xu, F. Synthesis of Upconversion $NaYF_4:Yb^{3+},Er^{3+}$ Particles with Enhanced Luminescent Intensity through Control of Morphology and Phase. *J. Mater. Chem. C* **2014**, *2*, 3671–3676.

(42) Krämer, K. W.; Biner, D.; Frei, G.; Güdel, H. U.; Hehlen, M. P.; Lüthi, S. R. Hexagonal Sodium Yttrium Fluoride Based Green and Blue Emitting Upconversion Phosphors. *Chem. Mater.* **2004**, *16*, 1244–1251.

(43) Mai, H.-X.; Zhang, Y.-W.; Si, R.; Yan, Z.-G.; Sun, L.; You, L.-P.; Yan, C.-H. High-Quality Sodium Rare-Earth Fluoride Nanocrystals:

Controlled Synthesis and Optical Properties. *J. Am. Chem. Soc.* **2006**, *128*, 6426−6436.

(44) Guo, H.; Yu, H.; Lao, A.; Chang, L.; Gao, S.; Zhang, H.; Zhou, T.; Zhao, L. Investigation of Sensitizer Ions Tunable-distribution in Fluoride Nanoparticles for Efficient Accretive Three-center Energy Transfer. *J. Appl. Phys.* **2014**, *116*, 103503.

(45) Kim, J. W.; Mackenzie, J. I.; Clarkson, W. A. Influence of Energy-Transfer-Upconversion on Threshold Pump Power in Quasi-Three-Level Solid-State Lasers. *Opt. Express* **2009**, *17*, 11935−11943.

(46) Boivin, D.; Föhn, T.; Burov, E.; Pastouret, A.; Gonnet, C.; Cavani, O.; Collet, C.; Lempereur, S. Quenching Investigation on New Erbium Doped Fibers Using MCVD Nanoparticle Doping Process. *Proc. SPIE* **2010**, *7580*, 75802B−1−75802B−9.

(47) Lock, M. P. E.; Andrews, D. L.; Jones, G. A. On the Nature of Long Range Electronic Coupling in a Medium: Distance and Orientational Dependence for Chromophores in Molecular Aggregates. *J. Chem. Phys.* **2014**, *140*, 044103.

(48) Andrews, D. L.; Harlow, M. J. Phased and Boltzmann-Weighted Rotational Averages. *Phys. Rev. A* **1984**, *29*, 2796−2806.

(49) Jiang, T.; Qin, W.; Zhou, J. Controllable Synthesis and Crystal Structure Determined Upconversion Luminescence Properties of Tm^{3+} (Er^{3+}) Ions Doped YbF_3 and $NaYbF_4$ Crystals. *J. Alloys Compd.* **2014**, *593*, 79−86.